Journal of Physics: Conference Series

Partial Coherence: a Route to Performing Faster Coherent Diffraction Imaging

To cite this article: Bo Chen *et al* 2013 *J. Phys.: Conf. Ser.* **463** 012033

11th International Conference on X-ray Microscopy (XRM2012) IOP Publishing
Journal of Physics: Conference Series **463** (2013) 012033 doi:10.1088/1742-6596/463/1/012033

Partial Coherence: a Route to Performing Faster Coherent Diffraction Imaging

Bo Chen[1,2*], Brian Abbey[1,3,4], Ruben Dilanian[1,2], Eugeniu Balaur[1,3], Grant van Riessen[1,3], Mark Junker[1,3], Chanh Q. Tran[1,3], Michael W.M. Jones[1,3], Ian McNulty[5], David J. Vine[5], Corey T. Putkunz[1,2], Harry M. Quiney[1,2], Keith A. Nugent[1,2,6]

[1] Australian Research Council Centre of Excellence for Coherent X-ray Science (CXS), Victoria, Australia
[2] School of Physics, The University of Melbourne, Victoria 3010, Australia
[3] Department of Physics, La Trobe University, Victoria 3086, Australia
[4] Melbourne Centre for Nanofabrication, 151 Wellington Road Clayton, Victoria 3168, Australia
[5] Advanced Photon Source, Argonne National Laboratory, Argonne, Illinois 60439, USA
[6] Australian Synchrotron, 800 Blackburn Rd, Clayton, Victoria 3168, Australia

E-mail: `boc@unimelb.edu.au`

Abstract. Coherent diffraction imaging (CDI) typically requires that the light source should be highly coherent both laterally and longitudinally. Beamlines at synchrotrons usually install a monochromator and slits to achieve a highly coherent source, leading to a large reduction of beam flux. We demonstrate that lateral and longitudinal partial coherence can be successfully included in a CDI reconstruction algorithm simultaneously, reducing the associated exposure time by two orders of magnitude. For the experimental case we present this allows the acquisition of CDI data in just 5 seconds compared to 20 minutes for full coherence. This significantly reduces the requirements on the stability of the imaging system as well as providing a route to imaging samples in real-time.

1. Introduction

With the development of modern X-ray sources such as third-generation synchrotrons and X-ray Free Electron Lasers (XFELs), many new forms of X-ray microscopy have been developed making it an area of active research. One of the most promising methods to be recently demonstrated is coherent diffraction imaging (CDI). Since its first demonstration using synchrotron radiation [1], CDI has been widely investigated and has found applications in material and biological sciences [2–4]. In principle, the resolution of CDI is not limited by the fabrication of X-ray optics, but by the experimental geometry. In practice, however, the resolution decreases as the 4th power with respect to incident flux, so much longer exposure times are required to achieve the highest resolution images [5].

Conventional CDI requires the source to be highly coherent both laterally and longitudinally. To achieve this, slits and a monochromator are installed at the beamline to give high coherence for the CDI experimental setup. The result of conditioning the beam in this way is a very significant loss of flux. Due to this decrease of flux, it usually takes tens of minutes to obtain high-resolution CDI experimental data, so that the requirement for stability of the experimental system is high, preventing the investigation of samples in real time. Recently, it has been found that the use of a modified reconstruction algorithm including *a priori* knowledge of the spectrum means that the monochromator can be removed from the system for CDI [6, 7]. In this method, the source is modeled as the combination of many monochromatic coherent modes of different frequency with the diffraction of each frequency component weighted and combined in the detector plane. This method still requires that the lateral coherence of the source is high. For a real source, however, the lateral coherence length is not always necessarily larger than the dimensions of sample. So, in many cases, the sample is illuminated with a partially coherent source, which will blur the diffraction pattern and cause the image reconstruction to fail. [8, 9].

In this paper, we demonstrate simultaneous use of partial lateral and partial longitudinal coherence in CDI and reduce the exposure time significantly to achieve real-time CDI.

2. Reconstruction Algorithm and Methods

The fundamental theory upon which partially coherent CDI is based can be found in [10, 11]. Here we provide a summary of the partially coherent CDI reconstruction algorithms. The notations are defined as follows. $\mathbf{r}$ and $\mathbf{r}'$ are any vectors in the sample and detector plane respectively, ν is the

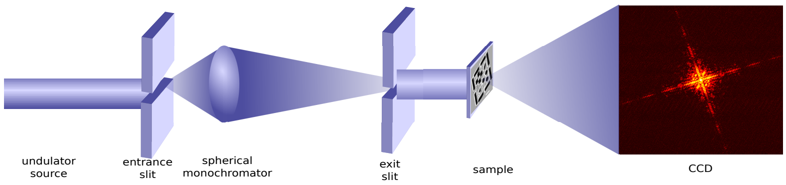

Figure 1. Schematic of the experimental setup. The diffraction pattern of the sample is shown on the right(in logarithmic scale).

frequency of the incident light with ν_0 the frequency at the peak of the spectrum, integer n is the mode number.

(i) Extract the coherent modes $\phi_n(\mathbf{r})$ from the source [12];

(ii) Fix at the peak spectrum $S(\nu_0)$, propagate the transmission function of the sample $T(\mathbf{r})$ with all the coherent modes $\phi_n(\mathbf{r})$, and calculate $I_n(\mathbf{r}', \nu_0) = |\phi_n(\mathbf{r})|^2$. The dominant coherent mode $\phi_0(\mathbf{r})$ results in the far field $\psi_0(\mathbf{r}')$;

(iii) Calculate the intensity $I(\mathbf{r}', \nu_0) = \sum_{n=0}^{N} \eta_n I_n(\mathbf{r}', \nu)$ with η_n the occupancy of coherent mode $\phi_n(\mathbf{r})$;

(iv) Scale the intensity with other frequency to calculate $I(\mathbf{r}', \nu)$;

(v) Sum the intensity with$I(\mathbf{r}') = \int S(\nu) I(\mathbf{r}', \nu) \mathrm{d}\nu$ to get the total calculated intensity $I_c(\mathbf{r}')$;

(vi) Use the measured intensity $I_m(\mathbf{r}')$ and calculated intensity $I_c(\mathbf{r}')$ to constrain the intensity, and use the phase $\psi_0(\mathbf{r}')$; $\psi(\mathbf{r}') = \sqrt{I_m(\mathbf{r}')}\psi_0(\mathbf{r}')/\sqrt{I_c(\mathbf{r}')}|\psi_0(\mathbf{r}')|$

(vii) Propagate $\psi(\mathbf{r}')$ back to sample plane by inverse Fourier Transforming and divide $\phi_0(\mathbf{r})$ to get the transmission function of the sample $T(\mathbf{r}) = \mathrm{FT}^{-1}\{\psi(\mathbf{r}')\}/\phi_0(\mathbf{r})$

(viii) Use sample plane constraint to get a new guess $T(\mathbf{r})$;

(ix) Repeat ii-viii until $\Omega = \sqrt{\sum_{\mathbf{r}'}[I_m(\mathbf{r}') - I_c(\mathbf{r}')]^2} / \sqrt{\sum_{\mathbf{r}'} I_m^2(\mathbf{r}')}$ is less than a given value.

Sample plane constraint such as error-reduction(ER), hybrid-input-out (HIO) [13] can be used as what has been done in traditional CDI.

3. Experimental results

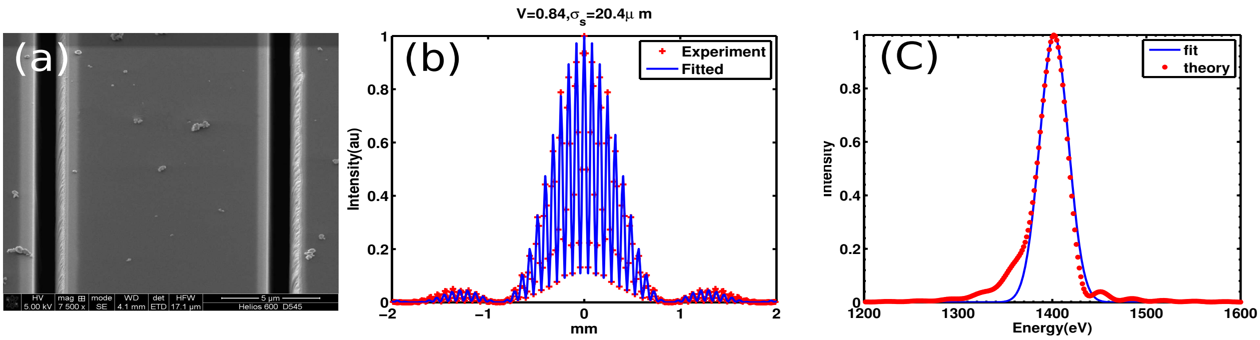

Figure 2. (a)The SEM image of the double slit fabricated with Focused Ion Beam (FIB).(b)The measured interference pattern of the double slit and fitted data when the incident beam is monochromatic and highly coherent.(c)The spectrum of the first order from the undulator at 2ID-B beamline of APS and a Gaussian fitting to this spectrum. The peak is at 1400eV. Theoretical data was calculated with SPECTRA developed by Takashi Tanaka and Hideo Kitamura, SPring-8/RIKEN.

Fig.1 shows a the schematic of the experimental setup. The experiment was carried out at the 2-ID-B beamline at the Advanced Photon Source (APS) [14] using conventional CDI. An x-ray beam with peak energy of 1.4 keV was used. The longitudinal coherence was controlled by the exit slit, while

slit setup(μm)	σ_s(μm)	σ(eV)	exposure time(s)
20/5	20.4	0.88	2
20/100	15.5	1.27	0.12
20/250	15.1	1.30	0.06
20/330	14.2	2.00	0.04
20/450	13.7	2.60	-
50/5	16.6	1.60	0.26
50/100	15.5	2.10	0.03
50/250	14.5	3.00	0.018
50/330	13.9	4.00	0.01
200/5	18.5	2.00	0.09
200/100	14.8	5.00	0.01
200/250	12.5	1.00	0.005
400/5	19.0	6.50	0.14
400/100	16.2	9.00	0.012
pink/5	12.3	15.08	10*
pink/100	10.8	15.08	1*
pink/250	9.9	15.08	0.5*
pink/330	9.5	15.08	0.4*
pink/450	9.0	15.05	0.5*

Table 1. The entrance and exit slit combinations used and the corresponding coherence length and bandwidth. The exposure time is for the diffraction data. "-" means the diffraction data is not available due to saturation, "*" means kapton film was used when taking the diffraction imaging. The thickness of the film is 51μm, the transmission at 1400eV is 3.94×10^{-4}, so the effective exposure time is the real exposure time by 3.94×10^{-4} . The effective exposure time for pink/450 is larger than pink/330, which may be due to the drop of the flux of the incident beam.

the lateral coherence was controlled by the entrance slit. A pair of Young's double slit and sample were installed in the same sample stage after a beam defining aperture (BDA) in the vacuum chamber. The CCD was sitting at 1057 ± 1mm downstream from the sample plane, with 2048×2048 pixels, each pixel $13.5 \times 13.5\mu\text{m}^2$. In our experiment, the separation of the double slits was $d = 11.75 \pm 0.25\mu$m, with the width of each slit $w = 1 \pm 0.03\mu$m.

In the experiment, we first closed the entrance slit to 20μm and used a monochromator to filter the beam and fitted the parameters of the slit. From the fitting, the real separation of the double slit is $d = 11.57\mu$m, the width of each slit $w = 1.02\mu$m, and the visibility is 0.84, so the coherence length $\sigma_s = 20.4\mu$m. In the case that the exit slit is fully open or the monochromator is not used, the longitudinal partial coherence is not negligible and must be included in the fitting. As a good approximation, we can fit the spectrum with a Gaussian function, even when there is no monochromator, as shown in Fig.2(b). In the experiment, we used several combinations of entrance and exit slit. For every combination, we first measured the interference pattern by translating the double slit into the beam, and then exchanging it with a fabricated sample, with the slits removed, to take diffraction data. To avoid saturation of the CCD, we keep the maximum counts to about 45000 for every frame of data; we summed 600 frames for every dataset presented here. The coherence properties of the source for every entrance and exit slit combination is fitted using the fitting methods [15] and is tabulated in Table 1. The fastest speed of the shutter is 0.005s, in some combinations, we had to attenuate the beam by installing a kapton film with thickness of 51μm in front of the CCD due to the shutter speed being too slow in comparison to the time for the CCD to saturate. This is equivalent to decreasing the flux by a factor of 3.94×10^{-4}. From the table we can see that the effective exposure time of partial coherence data is significantly smaller than that of the full coherence data. The exposure time of the 'pink'/5 setup is about 1/250 of that of 20/5 setup, which means the CDI experiment time was reduced from 20 minutes to just a few seconds. The effect of this major reduction in exposure time is to also decrease the stability requirements of the experimental setup.

The sample is fabricated on a gold film with thickness of 6μm with a focused ion beam (FIB). The size along the diagonal direction is 11.57μm. Because the size of holes in the sample is around 1μm, which is much smaller than the thickness, the walls of the triangular structure are not perpendicular to the surface and it barely extends through the film. The transmission through the gold sample at 1400eV is negligible, such that to a good approximation, it may be treated as a binary object with transmission function comprising only an amplitude component.

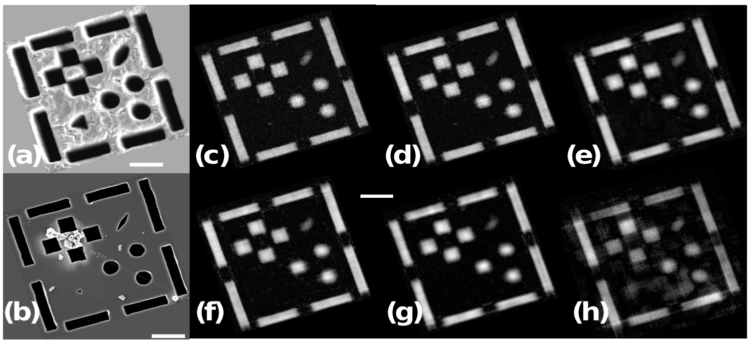

Figure 3. (a-b)The scanning electron microscopy image of the sample at (a) the front side and (b) the back side.(c-h) Reconstructed amplitudes of the sample for different entrance and exit slit combinations with our algorithm. (c) 20/5μm; (d) 20/250μm; (e) 50/5μm; (f) 200/100μm; (g) pink/5μm; (h) pink/100μm. Because the sample is thick relative to the size of the structures, the triangle is not fully penetrated. The scale bar is 2μm.

We reconstructed the sample with different slit combinations, as shown in Fig.3. We can see that by including the partial coherence in the reconstruction, the reconstruction works until at some instances, the data is blurred so much that the algorithms fails. The limit of the algorithm has been investigated elsewhere [11].

4. Conclusion

In this paper, we have demonstrated a partially coherent diffractive imaging method that includes both lateral and longitudinal coherence simultaneously in the reconstruction. This method leads to a two-orders of magnitude reduction in the exposure time for the sample examined compared to traditional CDI and makes much faster CDI experiments possible without loss of quality. It also reduces the stability requirement for the CDI system. With the use of recently developed fast-read detector technology, CDI it should be possible to image samples in real time in the future.

Acknowledgments

The authors acknowledge the support of the Australian Research Council Centre of Excellence for Coherent X-ray Science. Use of the Advanced Photon Source was supported by the US Department of Energy, Office of Science, Office of Basic Energy Sciences(contract no. DE-AC02-06CH11357).

References

[1] Miao J, Charalambous P, Kirz J and Sayre D 1999 *Nature* **400** 342–344
[2] Miao J, Nishino Y, Kohmura Y, Johnson B, Song C, Risbud S and Ishikawa T 2005 *Phys. Rev. Lett.* **95** 085503
[3] Robinson I and Harder R 2009 *Nature Materials* **8** 291–8
[4] Huang X, Nelson J, Kirz J, Lima E, Marchesini S, Miao H, Neiman A, Shapiro D, Steinbrener J, Stewart A, Turner J and Jacobsen C 2009 *Phys. Rev. Lett.* **103** 198101
[5] Shen Q, Bazarov I and Thibault P 2004 *J. Synchrotron Radiat.* **11** 432–8
[6] Chen B, Dilanian R A, Teichmann S, Abbey B, Peele A G, Williams G J, Hannaford P, Van Dao L, Quiney H M and Nugent K A 2009 *Phys. Rev. A* **79** 23809
[7] Abbey B, Whitehead L W, Quiney H M, Vine D J, Cadenazzi G A, Henderson C A, Nugent K A, Balaur E, Putkunz C T, Peele A G *et al.* 2011 *Nature Photonics* **5** 420–424
[8] Whitehead L W, Williams G J, Quiney H M, Vine D J, Dilanian R A, Flewett S, Nugent K A, Peele A G, Balaur E and McNulty I 2009 *Phys. Rev. Lett.* **103** 243902
[9] Clark J, Putkunz C, Curwood E, Vine D, Scholten R, McNulty I, Nugent K and Peele A 2011 *Opt. Lett.* **36** 1954–1956
[10] Williams G, Quiney H, Peele A and Nugent K 2007 *Phys. Rev. B* **75** 104102
[11] Chen B, Abbey B, Dilania R, Balaur E, van Riessen G, Junker M, Tran C, Jones M, Peele A, McNulty I, Vine D, Putkunz C, Quiney H and Nugent K 2011 *Phys. Rev. B* **86** 235401
[12] Starikov A and Wolf E 1982 *J. Opt. Soc. Am.* **72** 923–928
[13] Fienup J R 1982 *Appl. Opt.* **21** 2758–2769
[14] McNulty I, Khounsary A, Feng Y P, Qian Y, Barraza J, Benson C and Shu D 1996 *Rev. Sci. Instrum.* **67** 3372
[15] Paterson D, Allman B E, McMahon P J, Lin J, Moldovan N, Nugent K A, McNulty I, Chantler C T, Retsch C C, Irving T H K and Mancini D C 2001 *Optics Communications* **195** 79–84